Low-Lying Levels of ^{208}Pb with $g_{9/2}$, $i_{11/2}$, or $j_{15/2}$ Neutron-Particle Configurations*

PATRICK RICHARD,† P. VON BRENTANO,‡ H. WEIMAN, AND W. WHARTON
University of Washington, Seattle, Washington 98105
AND
W. G. WEITKAMP,§ W. W. MCDONALD, AND D. SPALDING
University of Pittsburgh, Pittsburgh, Pennsylvania 15213

(Received 3 February 1969)

The low-lying states of ^{208}Pb which have a neutron configuration $(g_{9/2}, j^{-1})$ are studied in proton scattering at the resonance energy for the $g_{9/2}$(g.s.) single-neutron isobaric-analog resonance (IAR) in ^{209}Bi. The on-resonance proton angular distributions are taken from 15° to 170° for states between 3.0- and 4.5-MeV excitation in ^{208}Pb, and are found to be nearly symmetric about 90° except for the lowest 5^- (3.192-MeV) state. Total proton inelastic scattering cross sections and proton partial widths are obtained from the angular distributions. The states in the energy ranges 3.0–3.8, 3.8–4.15, and 4.15–4.8 MeV in ^{208}Pb are found to have the dominant neutron–neutron-hole configurations of $(g_{9/2}, p_{1/2}^{-1})$, $(g_{9/2}, f_{5/2}^{-1})$, and $(g_{9/2}, p_{3/2}^{-1})$, respectively. Some tentative spin assignments based on the partial widths, excitation energy, and angular distributions of the states are given. Two previously unreported states at 3.940 and 4.376 MeV in ^{208}Pb are observed in the high-resolution (p, p') spectrograph data, and the levels previously reported at 4.032 and 4.252 MeV are observed to be doublets with 12- and 6-keV energy separations, respectively. The cross sections were also measured for the (p, p') reaction at the $g_{9/2}$ resonance at 20°, 40°. 60°, and 90° for 24 states between 4.6- and 6.00-MeV excitation. In addition to the $g_{9/2}$ resonance, the $i_{11/2}$(0.79-MeV) IAR and $j_{15/2}$(1.42-MeV) IAR are studied, and the observed states are compared with those observed in the ^{207}Pb(d, p) reaction. Partial widths for all the states between 2.0- and 4.5-MeV excitation containing $g_{9/2}$ neutron strength are calculated using the theoretical shell-model wave functions of Kuo and Brown and of Pinkston and True, and are compared with the experimentally observed widths.

I. INTRODUCTION

THE doubly magic ^{208}Pb nucleus offers one of the best cases for studying the matrix elements for the residual two-body interactions in nuclear shell-model calculations as witnessed by the large energy gap and the simple one-nucleon energy level schemes in ^{209}Pb,[1,2] ^{207}Pb,[2] ^{207}Tl,[3] and ^{209}Bi.[4] Because of the simple system of one nucleon built on the ^{208}Pb core, the low-lying levels of ^{208}Pb are expected to be described fairly well by neutron and proton particle-hole configurations. Shell-model calculations for these types of states have recently been performed.[5,6] Some proton particle-hole configurations have been investigated experimentally in the ^{209}Bi$(t, \alpha)^{208}$Pb reaction,[7] and some neutron particle-hole configurations have been studied in the ^{207}Pb$(d, p)^{208}$Pb reaction.[8] This paper treats in more detail the neutron particle-hole configurations excited in the proton decay of the analog states of ^{209}Pb.[9–13]

The isobaric-analog resonances (IAR) of the single-neutron states of ^{209}Pb have been studied in elastic scattering by several groups,[9–12] and the on-resonance inelastic scattering has been shown to excite selectively bands of states[11,13] in ^{208}Pb which consist of neutron particle-hole configurations. In particular, it has been shown that in the decay of the single-particle analog resonance in ^{209}Bi with spin J, states with the dominant configurations $(J, p_{1/2}^{-1})$, $(J, f_{5/2}^{-1})$, and $(J, p_{3/2}^{-1})$ are preferentially excited. An extensive study of the inelastic scattering excitation functions has been recently published. It has allowed us to determine which states in ^{208}Pb are resonating at analog resonances.[14] From this work and an earlier study,[11] the

* Supported in part by the U.S. Atomic Energy Commission and by the National Science Foundation.

† Present address: University of Texas, Austin, Tex. 78712.

‡ While on leave from and presently at Max Planck Institut für Kernphysik, Heidelberg, Germany.

§ Present address: University of Washington, Seattle, Wash. 98105.

[1] G. Muehllehner, A. S. Poltorak, W. C. Parkinson, and R. H. Bassel, Phys. Rev. **159**, 1039 (1967); M. Dost, W. R. Hering, and W. R. Smith, Nucl. Phys. **A93**, 357 (1967); G. M. Crawley, B. V. Narasimka Roe, and D. L. Powell, *ibid.* **A112**, 223 (1968).

[2] P. Mukherjee and B. L. Cohen, Phys. Rev. **127**, 1284 (1962).

[3] S. Hinds, R. Middleton, J. H. Bjerregaard, O. Hansen, and O. Nathan, Nucl. Phys. **83**, 17 (1966).

[4] R. Woods, P. D. Barnes, E. R. Flynn, and G. J. Igo, Phys. Rev. Letters **19**, 453 (1967); B. H. Wildenthal, B. M. Preedom, E. Newman, and M. R. Cates, *ibid.* **19**, 960 (1967); J. S. Lilley and N. Stein, *ibid.* **19**, 709 (1967); J. Bardwick and R. Tickle, Phys. Rev. **171**, 1305 (1968).

[5] Kuo and Brown (private communication). Because of the complexity of comparing signs as well as magnitudes of the wave-function configurations in these unpublished calculations to the data, we omit the comparison of the signs in Sec. IV.

[6] Pinkston and True (private communication). See also Ref. 5.

[7] J. H. Bjerregaard, O. Hansen, O. Nathan, R. Chapman, and S. Hinds, Nucl. Phys. **A107**, 241 (1968).

[8] J. Bardwick and R. Tickle, Phys. Rev. **161**, 1217 (1967); M. Dost and W. R. Hering, Phys. Letters **26B**, 443 (1968).

[9] C. D. Kavaloski, J. S. Lilley, P. Richard, and N. Stein, Phys. Rev. Letters **16**, 807 (1966).

[10] G. H. Lenz and G. M. Temmer, Phys. Letters **24B**, 370 (1967); Nucl. Phys. **A112**, 625 (1968).

[11] C. F. Moore, J. G. Kulleck, P. von Bretano, and F. Rickey, Phys. Rev. **164**, 1559 (1967).

[12] S. A. A. Zaidi, J. L. Parish, J. G. Kulleck, C. F. Moore, and P. von Brentano, Phys. Rev. **165**, 1312 (1968).

[13] N. Stein and D. A. Bromley, Phys. Rev. Letters **20**, 113 (1968).

[14] W. R. Wharton, P. von Brentano, W. K. Dawson, and P. Richard, Phys. Rev. **176**, 1424 (1968).

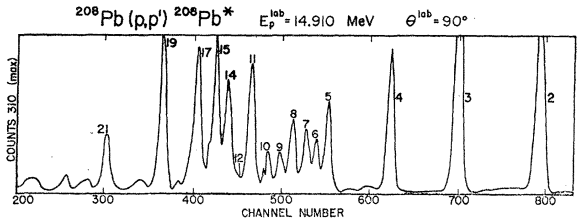

FIG. 1. Proton spectrum in the energy range 3.0–3.7-MeV excitation in ^{208}Pb taken with a 3 mm-Si(Li) detector at 90° at the $g_{9/2}$ resonance energy. The peak numbers in the figure are used in Table II. Resolution is 29-keV FWHM.

neutron particles J forming the neutron contribution to the neutron–neutron-hole configurations of the states in ^{208}Pb were determined.

In this paper, we give the on-resonance angular distribution for the $g_{9/2}$ resonance. From the angular distribution, one is able to obtain information about the neutron holes which make up the neutron–neutron-hole configurations. If one takes the information from the excitation functions together with the information from the angular distributions, one can determine completely, in principle, the various neutron–neutron-hole configurations which make up a given state. Since one obtains more than one solution for a given final state, spectroscopic factors from the (d, p) reaction help in determining the correct solution. One is in fact able, in principle, to get the relative signs as well as the magnitude of the coefficients for the various neutron–neutron-hole configurations in each state. Even in cases where the several configurations cannot be separated, one is able to obtain the total inelastic widths from the total cross section determined here, plus the parameters determined in Ref. 14. These widths can be compared with the predicted widths obtained (1) from shell-model calculations[5,6] of the ^{208}Pb wave functions and (2) from the experimental single-particle widths.[15,16] This technique has been used in the study of the low-lying levels of ^{206}Pb excited in the decay of the IAR of the single-hole states of ^{207}Pb.[17]

II. EXPERIMENTAL PROCEDURE

Proton beams of ~0.5 μA were obtained from the University of Washington three-stage FN Van de Graaff accelerator in the energy range 14–18 MeV. The beam was energy-analyzed by a 90° magnet and subsequently deflected by a switching magnet into a 60-in. scattering chamber. The targets used for this experiment were 99% enriched self-supporting Pb metal foils. The charged-particle spectra were obtained with 3-mm Si(Li) detectors, which were thermoelectrically cooled. Gold foils ~300 μg/cm^2 were placed in front of the detectors in order to eliminate electrons from the target. In addition, magnets were placed in front of the detectors for the purpose of removing electrons. Tennelec TC 130 preamplifiers[18] were used, followed by ORTEC 220 amplifier-bias amplifier systems.[19] Resulting pulses corresponding to 8–12-MeV particles were fed into ADC's and stored as 1024-channel spectra by the on-line SDS 930 computer. Other details of the experimental setup are given in Ref. 14.

The angular distributions were performed with two detectors. A third detector placed at 70° was used as a monitor detector. The energy resolution for these spectra ranged from 26 to 32 keV. Part of this resolution is due to target thickness (~10 keV for 10-MeV protons). A typical on-resonance spectrum is shown in Fig. 1 for the $g_{9/2}$ resonance.

Because of the count-rate problems in the solid-state detectors, it became increasingly difficult to obtain accurate angular distributions for the (p, p') reaction forward of 60°. Data were obtained as far forward as 15° by using the Enge split-pole spectrograph[20] and the three-stage EN Van de Graaff accelerator at the University of Pittsburgh. Photographic plates, used for recording the spectra, were scanned in 0.2-mm steps, and gave a resolution between 9 and 13 keV full width at half-maximum (FWHM). The absolute energy calibration for the ^{208}Pb(p, p') spectra was obtained by comparing it with energies given in Ref. 11. A spectrum for $\theta = 40°$ is given in Fig. 2. The small difference (40 keV) between the incident proton energies at which the Si(Li) data and the spectrograph data were taken is consistent with the combined uncertainties in the calibrations of the two accelerators and in the position of the $g_{9/2}$ IAR peak (FWHM = 253 keV).

Absolute cross sections were obtained by comparing the inelastic scattering with elastic scattering from the

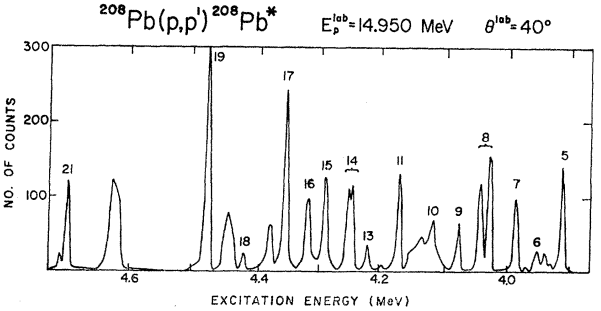

FIG. 2. Proton spectrum in the energy range 3.9–4.5-MeV excitation in ^{208}Pb taken at 40° with an Enge split-pole spectrograph at the $g_{9/2}$ resonance energy. The peaks are numbered the same as in Fig. 1. The resolution is 9-keV FWHM.

[15] D. J. Bredin, O. Hansen, G. H. Lenz, and G. M. Temmer, Phys. Letters **21**, 677 (1966).
[16] B. L. Anderson, J. P. Bondorf, and B. S. Madsen, Phys. Letters **22**, 651 (1966).
[17] P. Richard, N. Stein, C. D. Kavaloski, and J. S. Lilley, Phys. Rev. **171**, 1308 (1968).
[18] Tenneled Corp., Oak Ridge, Tenn.
[19] ORTEC, Inc., Oak Ridge, Tenn.
[20] B. L. Cohen, J. B. Moorehead, and R. A. Moyer, Phys. Rev. **161**, 1257 (1967).

same target at some low-energy and forward-scattering angle, where only Coulomb scattering is assumed to take place. For the Si(Li) data, the elastic scattering was taken at 5.0 MeV at angles between 50° and 90°, whereas for the spectrograph data, the elastic scattering was taken at 3.0 MeV and 38.0°.

III. ANALYSIS PROCEDURE

The proton decay via an inelastic scattering channel of an IAR of a pure single-neutron state of spin J leaves the final nucleus in a neutron–neutron-hole configuration of spin I.[11,12,14] All channel spins j which can couple to the particle spin J to form the final-state spin I are possible, but only the j values of the valence neutrons are allowed by the Pauli principle. The total proton inelastic width for a given state I is thus a sum over the partial widths for each j value:

$$\Gamma_{p'}=\sum_j \Gamma_{IjJ}{}^{p'}. \tag{3.1}$$

The angular distributions were fitted with an expression

$$(d\sigma/d\Omega)_{cc'}=A_0+A_2P_2+A_4P_4+A_6P_6. \tag{3.2}$$

The total inelastic scattering cross section for scattering from channel c to c' for an isolated resonance on a spin-zero target relates the value A_0 to the parameters Γ (total resonance width), Γ_{p_0} (elastic scattering partial width), E_0 (resonance energy), and $\Gamma_{p'}$ (partial width for channel c') by

$$\Gamma_{p'}=A_0[8k_p{}^2/(2J+1)\Gamma_{p_0}][(E-E_0)^2+\tfrac{1}{4}\Gamma^2], \tag{3.3}$$

where J is the spin of the resonance.

In order to give the connection between the experimental values of $\Gamma_{p'}$ obtained in this way and those predicted from theoretical wave functions, one has to use the S matrix as given, for example, by Weidenmüller[21–23]:

$$U_{cc}=U_{cc'}{}^D-\frac{ig_c{}^Jg_{c'}{}^J}{(E-E_0)+\frac{1}{2}i\Gamma}. \tag{3.4}$$

If the contributions from direct processes $U_{cc'}{}^D$ are neglected, then one obtains from this collision matrix an expression for the cross section[24,25]

$$d\sigma/d\Omega=\sum_L A_LP_L, \tag{3.5}$$

with

$$\frac{A_L}{A_0}=\frac{(-1)^{J-I}(2K+1)(2J+1)^{1/2}}{\Gamma_{p'}}C(JKJ\tfrac{1}{2}0\tfrac{1}{2})\times\sum_{j_1j_2}f(j_1j_2)C(j_1Kj_2\tfrac{1}{2}0\tfrac{1}{2})W(Jj_1Jj_2IK), \tag{3.6a}$$

where

$$f(j_1j_2)=(-1)^{j_1}(2j_1+1)^{1/2}\,\mathrm{Re}(g_{Ij_1J}{}^{p'}\times g_{Ij_2J}{}^{p'*}). \tag{3.6b}$$

The coupling schemes used in this formula are $0(\ell s)J$ and $I(\ell s)j$. The connection between the resonance amplitudes $g_c{}^J$ and the nuclear matrix elements is given[24]

$$g_{IjJ}(E_{p'})=g_j{}^{sp}(E_{p'})\langle(j\Psi_{I\alpha}{}^A)_J\,|\,\Psi_J{}^{A+1}\rangle. \tag{3.7}$$

In this formula, $\Psi_{I\alpha}{}^A$ and $\Psi_J{}^{A+1}$ stand for the antisymmetrized wave functions of the state $|I,\alpha\rangle$ and $|J\rangle$ in the residual nucleus and parent analog, respectively. If we expand the wave functions of the residual state in proton–proton-hole and neutron–neutron-hole configurations,

$$\Psi_{I\alpha}=\sum_{\alpha jJ}[a_{Ij\alpha}{}^J\nu(j^{-1},J)_I+b_{Ij\alpha}{}^J\pi(j^{-1},J)_I], \tag{3.8}$$

then we obtain from Eqs. (3.7) and (3.8)

$$g_{\alpha IjJ}=g_j{}^{sp}(E_{p'})\left(\frac{2I+1}{2J+1}\right)^{1/2}a_{Ij\alpha}{}^J. \tag{3.9}$$

In the application of Eq. (3.9), care must be taken that the coupling scheme and sign convention used in Eqs. (3.7) and (3.8) are the same as used in Eqs. (3.6). In terms of the partial widths, we have

$$\Gamma_{\alpha IjJ}=\Gamma_j{}^{sp}(E_{p'})\frac{2I+1}{2J+1}(a_{Ij\alpha}{}^J)^2, \tag{3.10}$$

where the single-particle widths $\Gamma_j{}^{sp}\equiv|g_j{}^{sp}|^2$ are the decay widths of a hypothetical single-particle analog resonance with spin J, which lies at an appropriate energy so as to give the correct channel energy. In our case, we have used such values from the decay of the 0^+ g.s. analog resonance in ^{208}Bi to the single-hole states in ^{207}Pb, and we have corrected these values for the channel energy by using Coulomb penetrabilities with the expression

$$\Gamma_j{}^{sp}(E_{p'})=\frac{P_j(E_{p'},R)}{P_j(E_{p'}{}^0,R)}\Gamma_j{}^{sp}(E_{p'}{}^0), \tag{3.11}$$

with $R=1.4A^{1/3}$ in units of f.

The above-mentioned values of $\Gamma_j{}^{sp}$ have been determined by Lenz and Temmer[10,15] and by Anderson, Bondorf, and Madsen.[16] We have actually used values of a more recent determination due to Grosse *et al.*,[26]

[21] H. Weidenmüller, Nucl. Phys. **A99**, 289 (1967).
[22] D. Robson and A. M. Lane, Phys. Rev. **161**, 982 (1967).
[23] A. F. R. de T. Piza and A. K. Kerman, Ann. Phys. (N.Y.) **43**, 363 (1967).
[24] J. P. Bondorf, P. von Brentano, and P. Richard, Phys. Letters **27B**, 5 (1968).
[25] D. Robson, in *Isospin in Nuclear Physics*, edited by D. H. Wilkinson [North-Holland Publishing Co., Amsterdam (to be published)]. The coupling scheme in this reference is $(sl)0J$ and $(sl)IJ$, as opposed to the one given in Ref. 24, which is used in this paper.
[26] E. Grosse *et al.* (private communication).

TABLE I. Legendre polynomial fit to angular distribution in ^{208}Pb(p, p') at 14.91-MeV incident proton energy.

E_{ex} (MeV)	$R(90°)$[a]	$R(90°)$[b]	A_0[c] (mb/sr)	A_2[c] (mb/sr)	A_4[c] (mb/sr)	χ^2
3.192	12	4	0.492±0.002	−0.051±0.004	−0.010±0.006	0.99
3.469	41	15	0.515±0.005	−0.187±0.007	−0.018±0.013	2.00
3.702	19	6.5	0.170±0.002	−0.123±0.004	0.035±0.005	2.15
3.913	59	10	0.137±0.002	−0.062±0.006	−0.013 0.008	1.13
3.955	30		0.058±0.002	−0.031±0.004	−0.024±0.006	1.25
3.992	26	8	0.106±0.002	−0.019±0.003	−0.020±0.005	2.99
4.032[d]	25	10	0.173±0.002	0.041±0.004	−0.021±0.005	1.10
4.080	2	1	0.050±0.002	−0.018±0.003	0.007±0.004	5.50
4.117	16		0.057±0.002	−0.032±0.003	−0.004±0.003	2.08
4.174	44	10	0.166±0.002	−0.108±0.004	0.002±0.005	1.17
4.225	...	...	0.034±0.001	0.009±0.002	0.008±0.003	2.17
4.252[d]	45	5	0.208±0.002	0.014±0.004	0.004±0.005	1.28
4.289	49	4	0.201±0.002	−0.124±0.004	0.001±0.005	1.40
4.351	38	10	0.255±0.003	−0.044±0.006	0.001±0.001	3.44
4.419	4	1.5	0.037±0.001	0.005±0.003	−0.002±0.004	3.66
4.475	34	10	0.321±0.002	0.099±0.004	−0.010±0.004	0.83
4.692	5	3	0.112±0.001	0.015±0.003	0.049±0.004	1.90

[a] $R(90°)$ is the ratio of the cross section at 14.2 MeV to that at 14.91 MeV for $\theta=90°$.

[b] $R(90°)$ is the ratio of the cross section at 15.67 MeV to that at 14.91 MeV for $\theta=90°$.

[c] A_0, A_2, and A_4 are the coefficients of the expansion $d\sigma/d\Omega=A_0P_0+A_2P_2+A_4P_4$ for $E_p=14.91$ MeV. A_6 is included in the analysis but not in the table.

[d] Doublets; see Table II.

which are, however, consistent with the earlier values

$$\Gamma_{p1/2}{}^{sp}(E_{p'}=11.49\text{ MeV})=28.6\text{ keV},$$
$$\Gamma_{f5/2}{}^{sp}(E_{p'}=10.92\text{ MeV})=4.2\text{ keV},$$
$$\Gamma_{p3/2}{}^{sp}(E_{p'}=10.59\text{ MeV})=15.8\text{ keV}, \quad (3.12)$$
$$\Gamma_{f7/2}{}^{sp}(E_{p'}=9.15\text{ MeV})=0.62\text{ keV}.$$

These values of $\Gamma_j{}^{sp}$ were derived from values of the expression $\Gamma_j{}^{sp}\Gamma_{g9/2}/\Gamma^2$, which are the quantities needed in this experiment. The quantities are accurate to better than 10%, which will allow us to rely quite heavily on the single-particle widths quoted.

IV. EXPERIMENTAL RESULTS AND DISCUSSION

A. $g_{9/2}$ Angular Distribution

A total of 23 states, including g.s. (0^+) and first excited state (3^-), are observed to resonate strongly at the $g_{9/2}$ resonance. The excitation functions are given in a previous publication,[14] but for the purpose of discussion, four of these are given in Fig. 3. As can be seen from this figure and also from the ratio of the resonance to the off-resonance cross section given in Table I, the cross section on resonance is almost entirely due to the resonance for nearly all states. This question has been treated for several states in more detail in the previous paper.[14] In the following, we will neglect the small direct amplitude completely, and will treat the on-resonance cross section as being due to the resonance only. The angular distributions for 17 of these states were obtained,[27] and the results of the Legendre polynomial fits of these angular distributions are given in Table I. These fits are based on the data from 60° to 170° obtained with the Si(Li) detectors. These data, together with the 15° to 90° spectrograph data, are displayed in Fig. 4. It might be expected that there would be considerable deviations from symmetry about 90° due to the interference of the resonance inelastic scattering with the direct (p, p') reaction. It is in fact observed that, at these bombarding energies, most of the angular distributions for states between 3.0- and 4.5-MeV excitation are nearly symmetric about 90°, the big exception being the 3.192-MeV (5^-) state. A detailed comparison of the forward-angle cross section with the best-fit curves of Table I is given in Fig. 5. From the values of A_0 given in Table I and the resonance parameters of Ref. 14, the values of $\Gamma_{p'}$ are obtained according to Eq. (3.3). These results are given in Table II, together with a comparison to the ^{207}Pb(d, p) results.[8] From the spectroscopic factors $(2I+1)S_{dp}$ determined in the

[27] P. Richard, W. G. Weitkamp, W. Wharton, H. Wieman, and P. von Brentano, Phys. Letters **28B**, 8 (1967).

^{207}Pb(d, p) reaction[8] and the single-particle widths, it is possible to calculate the width $\Gamma_{Ip1/2J}^{(d,p)} = \Gamma^{(d,p)}$ using Eq. (3.10). For the case of a state which contains only a single J, the value of $\Gamma^{(d,p)}$ should be smaller than the corresponding value $\Gamma_{p'}$, since $\Gamma_{p'}$ includes contributions from hole configurations other than $p_{1/2}$.

From the a coefficients [Eq. (3.8)] given by the wave-function calculations of Kuo and Brown[5] (KB) and from the single-particle widths [Eq. (3.12)] corrected for channel energy according to Eq. (3.11), we have calculated the proton partial widths using Eq. (3.10) for exciting the neutron–neutron-hole states in ^{208}Pb. The same procedure is used for calculating partial widths based on the wave functions of Pinkston and True[6] (PT). Figure 6 compares the experimental widths with the KB widths, and Fig. 7 compares the experimental widths with the PT widths. A rough comparison of the magnitude of the experimental widths with the theoretical widths shows fairly good agreement. By inspection, we see that PT predict the lowest 3^-, 5^-, 4^-, 5^- sequence much better than KB. In addition, the PT calculations show a spreading of states in excitation energy which resembles more closely the experimental data. It should be noted, however, that both calculations place the states about 200 keV higher than the observed ones.

B. Schematic Model

As discussed already, the proton width $\Gamma_{p'}$ of the states observed in the $g_{9/2}$ resonance is mainly due to the

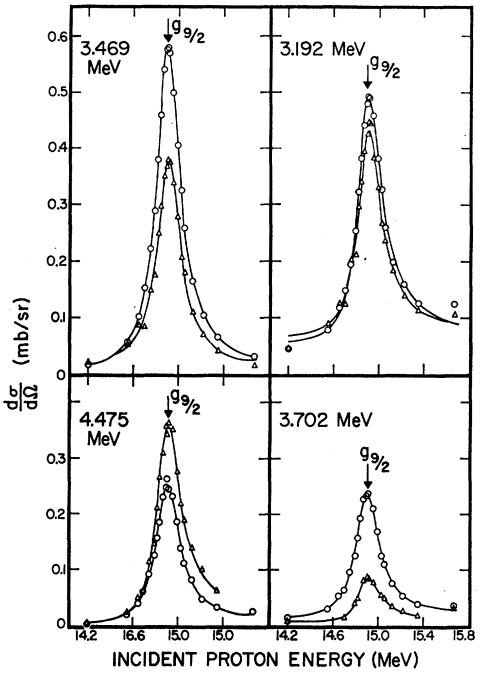

FIG. 3. Excitation functions for proton inelastic scattering near the $g_{9/2}$ IAR to the ^{208}Pb final states indicated. Circles represent 89.9° data, and triangles represent 149.3° data.

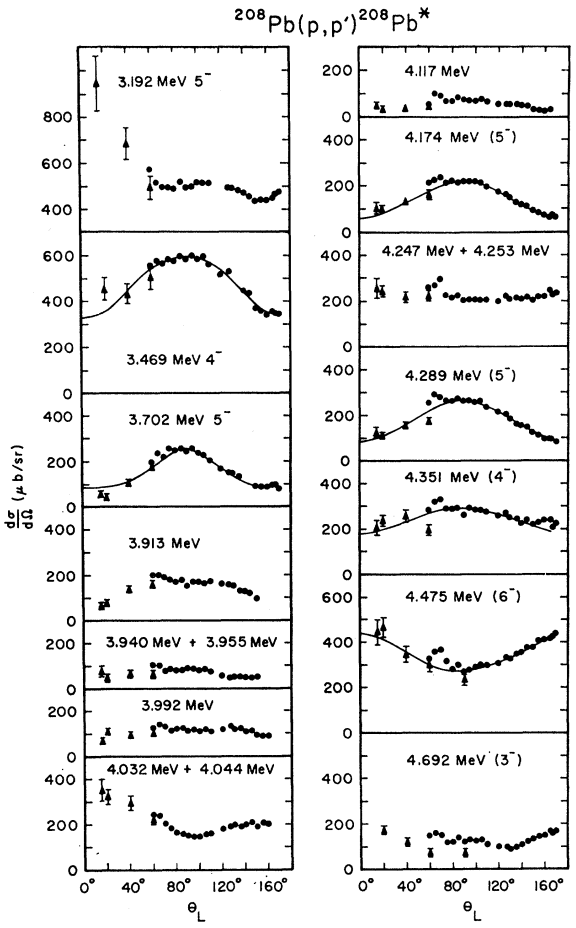

FIG. 4. Angular distributions for the inelastic scattering of protons (E_p=14.91 MeV) from ^{208}Pb at the position of $g_{9/2}$ IAR in ^{209}Bi. The solid curves for 4.175-, 4.289-, 4.351-, and 4.475-MeV states are for pure $(g_{9/2}p_{3/2}^{-1})$ neutron-neutron-hole configurations coupled to spins 5^-, 5^-, 4^-, and 6^-, respectively. The curves for the 3.469- (4^-) and 3.702-MeV (5^-) states represent the calculated cross sections for the neutron–neutron-hole configurations given in the text.

configurations $(g_{9/2}, p_{1/2}^{-1})$, $(g_{9/2}, f_{5/2}^{-1})$, and $(g_{9/2}, p_{3/2}^{-1})$. In a schematic model of ^{208}Pb, the multiplets of states with different spins, but belonging to a given configuration, are degenerate and lie at excitation energies E_x=3.430, 4.000, and 4.324 MeV, respectively. The energies, spins, decay widths, and angular distribution coefficients for these model states are given in Table III. In reality, the residual forces mix the various states of the schematic model. However, in the lead region this mixing is relatively weak, and we expect that the various multiplets will be mainly spread out in energy by the residual interaction and that different configurations will be mixed only relatively weakly. Exceptions to this are, of course, a few strong collective levels such as the 3^- 2.615-MeV state. In agreement with our expectation, the number of states with $\Gamma_{p'}>2$ keV is 14, whereas there are 12 states in the model. This shows that the mixing with other configura-

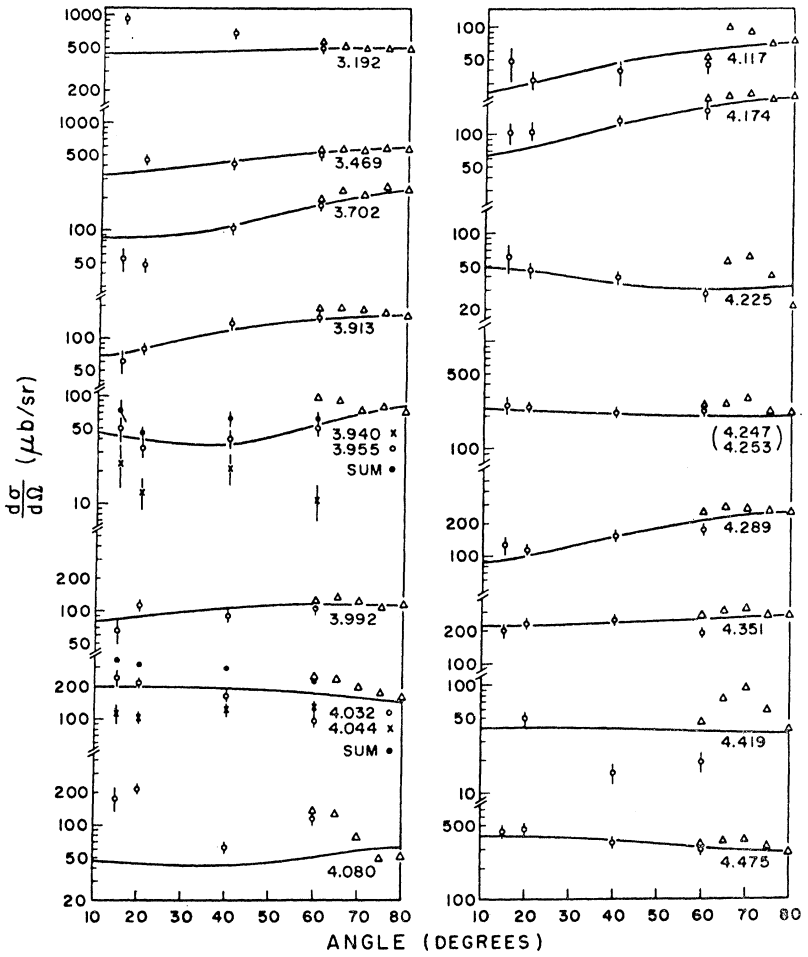

FIG. 5. Forward-angle data, with comparison of spectrograph data to the Si(Li)-detector data. The solid curves are calculated from the A coefficients in Table I.

tions, such as proton–proton-hole states, is weak, since we see only two additional states. Following our general expectations, we have divided the observed states in three groups which we believe to be mainly states with the configurations $(g_{9/2}, p_{1/2}^{-1})$, $(g_{9/2}, f_{5/2}^{-1})$, and $(g_{9/2}, p_{3/2}^{-1})$. This is shown in Table IV. As a check on these assumptions, we have investigated the validity of the sum rules for the states in the three groups. These sum rules should be strictly fulfilled if the multiplets do not mix:

$$\tilde{\Gamma}_{\alpha Ijj}=\frac{P_j(E_j^{\rm sp},R)}{P_j(E_{\alpha Ijj},R)}\,\Gamma_{\alpha Ijj}(E_{\alpha Ijj})=\Gamma_{\alpha Ijj}(E_j^{\rm sp}),\quad(4.1)$$

$$\sum_\alpha \tilde{\Gamma}_{\alpha Ijj}=(2j+1)\,\Gamma_j^{\rm sp},\quad(4.2)$$

$$\tilde{E}_{\rm expt}=\frac{1}{(2j+1)\,\Gamma_j^{\rm sp}}\sum E_{\alpha Ijj}\tilde{\Gamma}_{\alpha Ijj}=E_j^{\rm sp}.\quad(4.3)$$

In this relation, $E_j^{\rm sp}$ is the unperturbed energy of the multiplet. As can be seen from Table IV, these relations are fulfilled rather accurately for all three groups, and this leads us to assume that we have correctly identified the dominant configurations of the experimental states in the table.

The angular distribution for 3.469-MeV (4^-) state (Fig. 4) is not isotropic, as expected from the schematic model, so that a detailed analysis of the angular distribution of the states in the three groups is required. In Sec. IV C, the states in group I will be discussed, and in Secs. IV D and IV E, the states in groups II and III will be discussed.

C. 3.192–2.702-MeV States

1. 3.192-MeV (5^-) State

The 3.192-MeV (5^-) state does not have an angular distribution which is symmetric about 90°, as is seen in Fig. 4. The value $\Gamma_{p'}=22.9$ keV is obtained from the cross section backward from 90°. The value $\Gamma^{(d,p)}=28.0$ keV indicates that there may be some destructive interference at back angles in the (p, p') angular distribution, since $\Gamma^{(d,p)}$ should be less than or equal to $\Gamma_{p'}$. If the 5^- state were pure $p_{1/2}$ neutron hole, the observed width $\Gamma_{p'}$ would be 29.5 keV. KB predict a width of 14.3 keV, whereas PT predict 21.1 keV, which indicates more mixing of configurations in the

TABLE II. States observed with $g_{9/2}$, $i_{11/2}$, and $j_{15/2}$ neutron particle and results of comparison with ^{208}Pb(d, p).

No.[a]	E_{ex}[a] (MeV)	I^π	$(2I+1)S_{dp}$[b]	Neutron[b] configuration[b]	$\Gamma_{Ip_{1/2}J}{}^{(d,p)}$ [b] (keV)	$\Gamma_{p'}$[c] (keV)	J[c]
0	0.0	0^+					
1	2.608	3^-					
2	3.192	5^-	9.5	$g_{9/2}$	28.0	22.9	$g_{9/2}$
3	3.469	4^-	8.7	$g_{9/2}$	24.9	24.0	$g_{9/2}$
4	3.702	5^-	1.9	$g_{9/2}$	5.2	8.0	$g_{9/2}$
5	3.913	$(6^-, 7^-)$	...			6.5	$g_{9/2}$
	3.940		...			...	
6	3.955		...			2.7	$g_{9/2}$
7	3.992		...			5.1	$g_{9/2}$
8	4.032	$(7^-, 6^-)$	...			8.0	$g_{9/2}$
	4.044		...				
9	4.080	2^+	...			...	$g_{9/2}$
10	4.117		...			2.7	$g_{9/2}$
11	4.174	(5^-)	...			7.8	$g_{9/2}$
12	4.200					[d] ...	$i_{11/2}$
13	4.225					1.6	$g_{9/2}$
14	4.247		23.2	$i_{11/2}$	55.0	...	...
	4.253	(3^-)	0.6	$g_{9/2}$	1.5	9.7	$g_{9/2}$
15	4.289	(5^-)				9.4	$g_{9/2}$
16	4.317		...			...	$g_{9/2}$
17	4.351	(4^-)	...			12.0	$g_{9/2}$
	4.376		...			...	$g_{9/2}$
18	4.419	6^+	...			1.7	$g_{9/2}$
19	4.475	(6^-)	...			15.1	$g_{9/2}$
20	4.602		10.0	$j_{15/2}$	18.4	...	$j_{15/2}$
21	4.692	(3^-)	1.5	$d_{5/2}$	7.4	5.3	$g_{9/2}$, $i_{11/2}$, $d_{5/2}$
22	4.835		20.0	$j_{15/2}$	35.7	...	$j_{15/2}$
23	4.857						
24	4.928					...	$i_{11/2}$
27	5.071					...	$i_{11/2}$

[a] Excitation energies for the numbered states are taken from Ref. 11. Two new states at 3.940 and 4.376 are unnumbered. Doublets at 4.032 and 4.253 are indicated. The same numbering of states is used in Figs. 1 and 2.

[b] (d, p) results are taken from Ref. 8.

$$\Gamma_{Ip_{1/2}J}{}^{(d,p)} = [(2I+1)S_{dp}/(2J+1)]\,\Gamma_{1/2}{}^{sp}.$$

[c] Inelastic width for state I at resonance J includes contributions from all possible neutron holes j. The values J are obtained from the (p, p') excitation functions (Ref. 14).

[d] A 4.22–4.28-MeV doublet is analyzed in the (d, p) reaction at this energy region.

5^- than is observed. A detailed analysis of this state must await the proper resonance–direct-interference calculations. Nonetheless, this state does appear to exhaust much of the $p_{1/2}$ neutron-hole strength for 5^- states. This state is also known to contain 6% ($h_{9/2}$, $s_{1/2}{}^{-1}$) proton particle-hole strength, as measured in the ^{209}Bi$(t, \alpha)^{208}$Pb reaction.[7] In the ^{209}Bi$(d, {}^3$He) measurements made at Berkeley,[28] the ($h_{9/2}$, $s_{1/2}{}^{-1}$) strength was measured to be 8%.

[28] C. Glashausser, D. L. Hendrie, and E. A. McClatchie (private communication).

2. 3.469-MeV (4^-) State

The angular distribution which is symmetric about 90° for this state has been analyzed in detail elsewhere,[24] so the results will only be summarized here. From Eqs. (3.6), the values of A_k in Table I, and the (d, p) result that $a_{4-p1/2}{}^{9/2}\sim 0.98$ (Table II), we get the solution

$$a_1 = +0.94 \pm 0.02, \qquad a_5 = +0.07 \mp 0.16,$$

and

$$a_3 = -0.24 \pm 0.03.$$

TABLE III. Energies, widths, and angular-distribution coefficients for the neutron particle-hole states $(g_{9/2}, j^{-1})$ of ^{208}Pb in the absence of residual interactions.

E_{ex} [a] (MeV)	E_p c.m. [b] (MeV)	j	I	$\Gamma_{p'}$ [c] (keV)	A_2/A_0 [d]	A_4/A_0 [d]
3.430	11.417	$p_{1/2}$	5⁻	31.5	...	...
			4⁻	25.7	...	...
4.000	10.847	$f_{5/2}$	7⁻	6.30	0.520	0.054
			6⁻	5.45	−0.450	−0.282
			5⁻	4.62	−0.606	0.482
			4⁻	3.78	−0.260	−0.117
			3⁻	2.94	0.329	−0.507
			2⁻	2.10	0.952	0.428
4.324	10.524	$p_{3/2}$	6⁻	20.5	0.364	...
			5⁻	17.8	−0.606	...
			4⁻	14.4	−0.303	...
			3⁻	11.1	0.667	...

[a] As calculated from Ref. 2.

[b] These energies are the outgoing proton energies in the ^{208}Pb$(p, p')^{208}$Pb* reaction at the $g_{9/2}$ resonance, leading to the state of excitation energy given in column 1.

[c] These widths are calculated according to Eq. (3.9) with the use of the single-particle widths given in Eq. (3.11).

[d] It should again be noted that small admixtures of other configurations can change these values very much.

KB give for the lowest 4⁻ state wave function

$$|a_1|=+0.988, \quad |a_5|=+0.07, \quad \text{and} \quad |a_3|=+0.121,$$

whereas PT give

$$|a_1|=+0.962, \quad |a_5|=+0.21, \quad \text{and} \quad |a_3|=+0.163,$$

where a_{Ij}^{J} is denoted by a_{2j}. The magnitudes of the $p_{1/2}$ and $p_{3/2}$ configurations are seen to agree quite well with the theory, whereas the $f_{5/2}$ are not very well determined experimentally. Many proton particle-hole configurations can be eliminated, since the 3.469-MeV state is not excited in the ^{209}Bi(t, α) reaction[7] or the ^{209}Bi$(d, {}^3\text{He})$ reaction,[28] and many other neutron particle-hole configurations can be eliminated, since the 4⁻ does not resonate at the higher neutron single-particle resonances. The (d, p) data[8] yield a value $\Gamma_{4^-\,1/2^-\,9/2}{}^{p'}=22.6$ keV.

Angular distributions were taken above and below the $g_{9/2}$ resonance in order to establish the degree of deviation from the single-level Breit-Wigner shape. If there were no deviations, the ratios of A_2/A_0 and A_4/A_0 would be the same at all energies. The data are given in Fig. 8, and the results of the fit are given in Table V. The errors are larger for the off-resonance data, due to the smaller cross section. The ratios A_2/A_0 are nearly within experimental errors. These

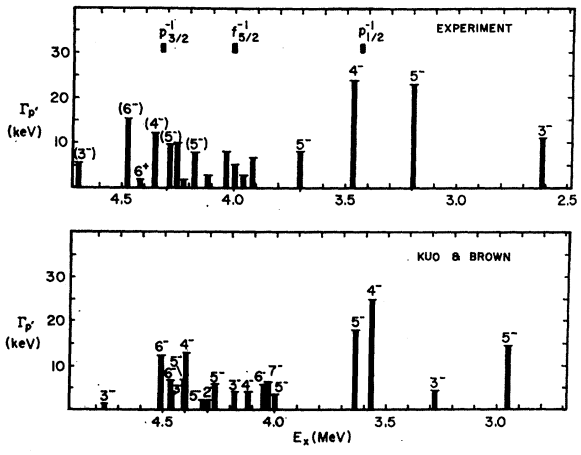

FIG. 6. Observed proton partial widths for the $g_{9/2}$ resonance, with a comparison to the $g_{9/2}$ neutron strength in ^{208}Pb as calculated by Kuo and Brown.

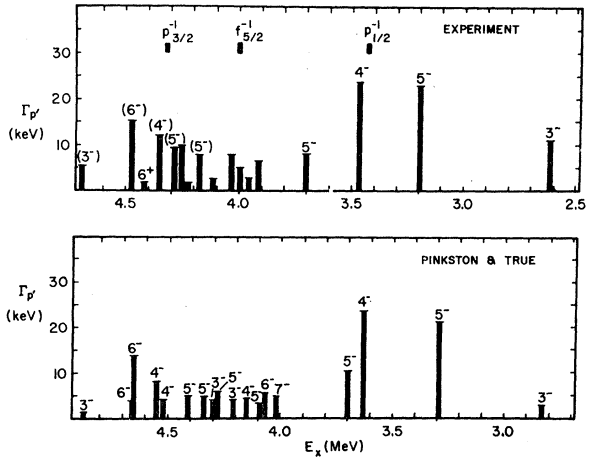

FIG. 7. Observed proton partial widths for the $g_{9/2}$ resonance, with a comparison to the $g_{9/2}$ neutron strength in ^{208}Pb as calculated by True and Pinkston.

TABLE IV. Schematic model of ^{208}Pb states.

	No. of states with $\Gamma_{p'}>2$ keV	E_{ex}^{min} to E_{ex}^{max} (MeV)	$\Sigma_{\alpha I}\tilde{\Gamma}_{IiJ}$ (keV)	Assigned configurations	$(2j+1)\Gamma_j^{sp}(E_j^{sp})$	$\tilde{E}_{expt}$ (MeV)	E_j^{sp} (MeV)
I	3	3.0–3.8	55.8	$g_{9/2}p_{1/2}^{-}$	57.2	3.375	3.430
II	5	3.8–4.15	25	$g_{9/2}f_{5/2}^{-}$	33	3.994	4.000
III	6	4.15–4.8	62.4	$g_{9/2}p_{3/2}^{-}$	56	4.37	4.324

results add confidence to the determined values of the $p_{1/2}$ and $p_{3/2}$ neutron-hole configurations of the 4^-, whereas the large error in the $f_{5/2}^{-1}$ configuration is further manifested in the deviations of A_4/A_0. If A_4 were zero, then $\Gamma_{4^-\,5/2^-\,9/2}$ would be exactly zero.

3. 3.702-MeV (5^-) State

In view of the excellent agreement between the (d, p) and (p, p') determination of the $p_{1/2}$ strength for the 4^- state, we begin the analysis of the 3.702-MeV (5^-) state by using the value $\Gamma^{(d,p)}=5.2$ keV$=\Gamma_{5^-\,1/2^-\,9/2}{}^{p'}$ (see Table II). As before, we consider only $p_{1/2}$, $f_{5/2}$, and $p_{3/2}$ contributions, so that from the observed $\Gamma_{p'}=8.0$ keV, the sum of the widths for $p_{3/2}(\Gamma_{3/2})$ and $f_{5/2}(\Gamma_{5/2})$ is 2.8 keV. Equations (3.6), together with the experimental A coefficients, yield the additional relations

$$A_2/A_0=-0.724=(-0.606/\Gamma_{p'})(\Gamma_{3/2}+\Gamma_{5/2}-2.76\sqrt{\Gamma_{5/2}}+4.46\sqrt{\Gamma_{3/2}}), \quad (4.4)$$

$$A_4/A_0=+0.206=(+0.482/\Gamma_{p'})\times(\Gamma_{5/2}-0.864\sqrt{\Gamma_{3/2}}\sqrt{\Gamma_{5/2}}). \quad (4.5)$$

The fortunate form of the equations allows us to substitute $\Gamma_{3/2}+\Gamma_{5/2}=2.8$ keV in Eq. (4.1) and $\Gamma_{p'}=8$ keV in Eqs. (4.1) and (4.2), so that we can easily solve the quadric equation in $\Gamma_{5/2}$ and the linear equation in $\sqrt{\Gamma_{3/2}}$. Of the two possible solutions, one gives an $f_{5/2}$ width much larger than the single-particle width, and is thus rejected. The other result gives

$$a_1=+0.41\pm0.02, \quad a_5=-0.76\mp0.12, \quad a_3=+0.10\mp0.18. \quad (4.6)$$

The coefficients given by PT for a 5^- state at 3.70 MeV are

$$|a_1|=+0.567, \quad |a_5|=+0.353, \quad |a_3|=+0.104, \quad (4.7)$$

whereas KB give for a 5^- state at 3.64 MeV

$$|a_1|=+0.747, \quad |a_5|=+0.275, \quad |a_3|=+0.134. \quad (4.8)$$

The magnitude of the coefficients does not agree very well with the theory. In particular, the calculated $f_{5/2}$ contribution is too small compared with the experimental one. In presenting this analysis we should, however, point out that the cross section to the 5^- 3.702-MeV state has a measurable direct component. Since we have neglected this component, the analysis presented, which was based on the assumption of pure compound cross section, may be erroneous.

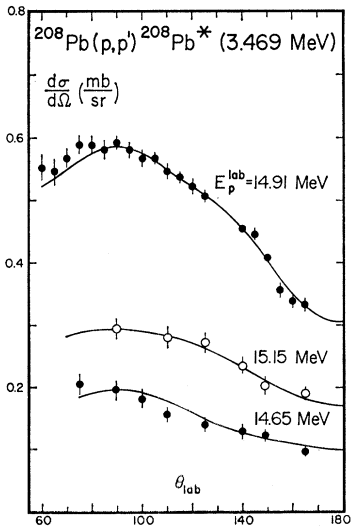

FIG. 8. Angular distributions for ^{208}Pb (4^-) state on and near the $g_{9/2}$ resonance.

D. 3.913–4.117-MeV States

The spins of the eight states in this region of excitation are not known, and thus a detailed analysis is not possible at this point. These states are expected to be mainly $(g_{9/2}, f_{5/2}^{-1})$ and thus should have widths in the range 7–2 keV (see Table III). The difficulty is that small admixtures of $p_{1/2}^{-1}$ and $p_{3/2}^{-1}$ greatly influence the magnitude of the cross sections as well as the angular distributions. Because of the spin factor,

TABLE V. Legendre polynomial fit to the ^{208}Pb(p, p') ^{208}Pb(3.469 MeV, 4^-) near the energy of the $g_{9/2}$ IAR.

E_p^{lab}	A_2/A_0		A_4/A_0		χ^2
14.650	−0.418	0.076	0.114	0.114	1.14
14.918	−0.364	0.015	−0.040	0.030	2.00
15.150	−0.305	0.045	0.037	0.045	1.50

the pure $f_{5/2}$ 7^- state has the largest cross section of the pure $f_{5/2}$ states and also cannot mix with $p_{1/2}$ or $p_{3/2}$ configurations. One would therefore expect this state to lie at about 4 MeV and to have an angular distribution similar to the one given in Table III. A_2/A_0 is positive for this state, so that the only state near 4 MeV which satisfies this condition is the 4.032-MeV doublet. This doublet is resolved only in the spectrograph data at forward angles and is plotted in Fig. 5. Since these states are barely resolved, the errors are rather large. PT predict a 7^- state at 4.02 MeV which is 98% $(g_{9/2}, f_{5/2}^{-1})$, and KB predict a 7^- state at 4.03 MeV which is 96% $(g_{9/2}, f_{5/2}^{-1})$. However, if the widths of the state in the doublet at 4.032 MeV are distributed as the forward cross sections indicate, then the strength of both falls slightly short of the 6.0 keV expected for a 7^- state. PT and KB predict a nearly pure 6^- state at 4.07 and 4.05 MeV, respectively. In this energy region the 3.913-MeV state has an A_2/A_0 value of -0.45, which agrees with the $(g_{9/2}, f_{5/2}^{-1})$ 6^- value given in Table III. The A_4/A_0 coefficient is not in good agreement, but does have the correct sign. In addition, the observed width of 6.5 keV is larger than the pure configuration value of 5.45 keV (Table III). In conclusion, it is not perfectly clear which of these two states discussed is 7^- or 6^-.

E. 4.174–4.69-MeV States

The strong states of this group have been assigned the dominant configuration $(g_{9/2}, p_{3/2}^{-1})$ in Table IV, and the expected value of $\Gamma_{p'}$ for pure $(g_{9/2}, p_{3/2}^{-1})$ configurations have been given in Table III. On the basis of these widths, the 4.475-MeV state must have a spin 6^- or 5^-. If we assume it to be a pure $(g_{9/2}, p_{3/2}^{-1})$ 6^-, 5^-, 4^- configuration then, from Eq. (3.10) and the sp width, we would expect it to have the width $\Gamma_{6^-\,1/2^-\,9/2}(E_{p'}=10.37)=19.5$ keV or $\Gamma_{5^-\,1/2^-\,9/2}(E_{p'}=10.37$ MeV$)=16.4$ MeV or $\Gamma_{4^-\,1/2^-\,9/2}(E_{p'}=10.37$ MeV$)=13.5$ keV, as compared with the experimental value of 15.1 keV. Thus we can rule out the spins 4^- and 3^- for this state. Both KB and PT predict, however, the 5^- states which have natural parity to be spread out more or less equally among two or three other states. Thus none of these 5^- states would have a width as large as the observed partial width. It seems reasonable, therefore, to assume that the 4.475-MeV state has indeed the spin $I=6$. The angular distribution of the state is indeed in agreement with a pure $(g_{9/2}, p_{3/2}^{-1})$ configuration, as shown in Fig. 4, but small amounts of $(g_{9/2}, p_{1/2}^{-1})$ could change a $(g_{9/2}, p_{3/2}^{-1})$ 5^- distribution very much, and thus one cannot make this argument rigorous. It would be very desirable to have a reliable upper estimate on a possible amplitude $(a_{5^-\,1/2^-\,9/2})^2$ in this state, as could be obtained from a (d, p) experiment, since this would allow us to make a unique assignment. The state with the next largest width is the 4.35-MeV state, which has $\Gamma_{p'}=12$ keV. Even though we expect the $(g_{9/2}, p_{3/2}^{-1})$ 5^- strength to be spread out among several states, we do expect that a $(g_{9/2}, p_{3/2}^{-1})$ 4^- state which has unnatural parity to be rather pure, so that we would assign the 4.35-MeV state the spin $I=4^-$. The expected width for a pure $(g_{9/2}, p_{3/2}^{-1})$ 4^- state is $\Gamma_{4^-\,1/2^-\,9/2}(E_{p'}=10.5)=14$ keV, which indeed is compatible with the experimental width $\Gamma_{p'}=12$ keV. Again we note that the angular distribution fits rather nicely, as shown in Fig. 4. Finally, we have four states at $E_x=4.174$, 4.289, and 4.253 MeV (doublet). Since the angular distributions of the 4.174- and 4.289-MeV states both agree exactly with a $(g_{9/2}, p_{3/2}^{-1})$ 5^- angular distribution (see Fig. 4), it is tempting to think they both have $I=5$. Further support for this assignment is based on the fact that the sum rule for the 5^- states gives for the energy-corrected widths $\Gamma_{p'}4.174$ $(E_{p'}=10.59)+\Gamma_{p'}4.289$ $(E_{p'}=10.59)=$ 16.85 keV, as compared with a sp limit of 17.8 keV. If we had made all these assumptions, then we would be forced to assign one of the 4.25-MeV states the spin 3, in order to account for the width $\Gamma_{p'}=9.7$ keV. The distribution of strength between these two states is not known, however; either one would probably fall short of the sp limit of 11.1 keV given in Table III. All these assignments, with the exception of the 6^- assignment to the 4.475-MeV state, are based on many assumptions and must be regarded with some suspicion. Recent investigations[29] of the ^{208}Tl (β^-) decay supports the 6^- and two 5^- spin assignments.

The 4.692-MeV state is observed to resonate at the $g_{9/2}$, $i_{11/2}$, and $d_{5/2}$ single-neutron IAR[12,14] and is observed in the ^{207}Pb(d, p) reaction.[8] From Figs. 6 and 7, we see that both PT and KB predict a 3^- state near this energy, and we thus make a spin assignment based on this comparison. The state has a large degree of collectivity, since it has a large off-resonance cross section. This alone indicates the state is probably a natural-parity state with $I=2^+$ or 3^-. Further evidence for the validity of the 3^- assignment will be given in a future publication, which deals with the $d_{5/2}$ through $d_{3/2}$ single-neutron analog resonance.[30]

F. 4.703–6.000-MeV States

The ^{208}Pb states in this region of excitation are expected to have small cross sections in the (p, p') reaction and to be closely spaced in energy. The neutron particle-hole strength $(g_{9/2}, j^{-1})$ is expected to be mainly due to $j=i_{13/2}$ and $j=f_{7/2}$, which have very small single-particle widths at the channel energies of 9.787 and 9.077 MeV, respectively. The excitation energies in ^{208}Pb in the absence of residual interactions are 5.06 and 5.77 MeV for the $i_{13/2}$ and $f_{7/2}$, respectively. Table VI contains the results of the forward-angle (p, p') data in this excitation region taken with the spectrograph. Many states with small cross sections are

[29] A. Pokkanen, J. Kantele, and P. Suominen, Z. Physik **218**, 273 (1969); H. Ostertag and K. H. Lauterjung, *ibid.* **199**, 25 (1967).

[30] P. von Brentano, P. Richard, and W. R. Wharton (unpublished).

TABLE VI. ^{208}Pb(p, p') ^{208}Pb*(4.5–6.0 MeV) cross sections on the $g_{9/2}$ IAR (cross sections in μb/sr). Errors are total uncertainties.

E_{ex}	20°	40°	60°	90°	90°[a]
4.475				232±23	225.4
4.692 (3$^-$)	174±20	121±15	77±16	77±9	93.6
4.703	18±18	14±5	23±10		
4.835	20±5	43±7	15±2	21±3	
4.857	24±6	3±3	2±2		
4.928	13±4	contaminant	3±2	8±2	
4.967	14±4	contaminant	9±2	18±2	29.0
5.030 (3$^-$)	58±12	19±6	12±4	5±1	
5.071	8±6	9±3	14±2	6±1	
5.121	14±4	3±2	7±2	8±1	
5.205	17±6	8±3	10±2	17±2	15.1
5.238 (3$^-$)	57±18	18±4	14±3	6±1	
5.284	38±7	10±5	18±3	20±2	26.6
5.338	34±6	10±3	12±8	14±6	
5.373	10±4	10±3	contaminant	17±4	(9.4)
5.474	47±9	9±3	contaminant	18±4	25.0
5.505	160±18	89±20	55±14	41±6	55.0
5.536	16±5	21±6	8±6	11±3	
5.554	14±8	34±10	6±2	10±2	18.7
5.646	13±8	14±4	17±5	15±3	23.0
5.679	36±8	19±8	34±10	27±5	42.5
5.769	11±6	40±14	0±2	1±2	
5.804	41±7	contaminant	10±2	14±3	
5.827	56±14	contaminant	10±3	12±3	
6.000	26±6	contaminant	16±4	12±2	

[a] Cross section taken from Ref. 11.

observed, and no analysis is attempted. The states at 4.692, 5.030, 5.238, and 5.505 MeV show strong forward-angle peaking. The 5.03-MeV state is observed to resonate at the $d_{5/2}$ resonance[14] and is also observed in the ^{207}Pb(d, p) reaction with a characteristic $d_{5/2}$ angular distribution which restricts the spin to 3$^-$ or 2$^-$. The forward-angle peaking of this state in this low-energy (p, p') reaction indicates that it is a natural-parity state and is thus a 3$^-$ state. This spin assignment implies a ($d_{5/2}$, $p_{1/2}^{-1}$) spectroscopic factor of 0.37.[8] The same argument can be made for the 5.238-MeV state.[11,29] An assignment of 3$^-$ for this state implies a ($d_{5/2}$, $p_{1/2}^{-1}$) spectroscopic factor of 0.198. From Table VI, note that the 4.692-MeV (3$^-$) state shows the expected forward-angle peaking. A state at 5.505 MeV has previously been assigned a spin 1$^-$ on the basis of its ground-state γ-decay strength.[31]

[31] J. G. Cramer, P. von Brentano, G. W. Phillips, H. Ejiri, S. M. Ferguson, and W. J. Braithwaite, Phys. Rev. Letters **21**, 297 (1968).

G. $i_{11/2}$ Isobaric-Analog Resonance

The states excited in the inelastic proton scattering at the $i_{11/2}$ IAR have small cross sections (~150 μb/sr) due to the angular momentum barrier for the i-wave protons in the entrance channel. Four states have cross sections large enough to allow extraction of an excitation function.[14] These states are the 4.200-, 4.692- (3$^-$), 4.928-, and 5.071-MeV states listed in Table II. Of these states, only the 4.200-MeV state is observed in the ^{207}Pb(d, p) reaction with an $i_{11/2}$ neutron transfer. This state, perhaps a doublet, is likely to be mainly ($i_{11/2}$, $p_{1/2}^{-1}$) on the basis of the single-particle energies which predict in the absence of residual interactions a 5$^-$ 6$^-$ doublet near 4.22 MeV.

The outgoing proton spin in the (p, p') excitation of the 4.692-MeV (3$^-$) state at the $i_{11/2}$ IAR cannot be $p_{1/2}$ or $p_{3/2}$, but can be $f_{5/2}$. It is somewhat surprising that this cross section is observable when the single-particle widths are considered. This state is observed in the (d, p) reaction, but only through the $d_{5/2}$ neutron transfer.

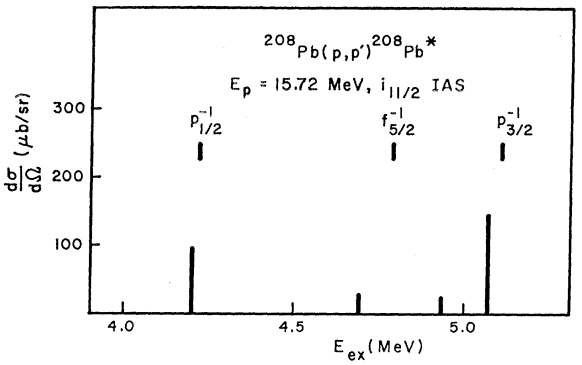

FIG. 9. Cross sections and energies for the states observed at the $i_{11/2}$ IAR are given here, together with the energy of the three lowest neutron holes. 90° cross sections are given for the 5.071- and 4.20-MeV states, whereas 158° cross sections are given for the 4.928-MeV state.

The remaining two observed states at 4.928 and 5.071 MeV lie near the zero energy (5.114 MeV) for $(i_{11/2}, p_{3/2}^{-1})$ configurations. These states are not observed in the (d, p) reaction, indicating very little mixing of $p_{1/2}$ hole strength. The 5.071-MeV state has the largest cross section of these states and is probably a high-spin member of the $(i_{11/2}, p_{3/2}^{-1})$ quartet, due to statistical factors.

Figure 9 displays the differential cross section at some angle for each of the four observed states and also compares the energies of these states with the three lowest single-neutron–hole energies. The proton partial widths were not analyzed, because of the large uncertainty in the elastic width for the $i_{11/2}$ IAR.

H. $j_{15/2}$ Isobaric-Analog Resonance

At the energy of the $j_{15/2}$ IAR, two states are observed to resonate with an extremely small cross section. The off-resonance cross section is $\sim 15\ \mu$b/sr, compared with $\sim 30\ \mu$b/sr on resonance. As in the case of $i_{11/2}$ IAR, this small cross section is due to the small value of the elastic width Γ_{p0}. The resonance is observed in the 4.602-MeV state and 4.835–4.857-MeV doublet. The same states are observed as $L=7$ neutron transfer states in the ^{207}Pb(d, p) reaction.[8] From this fact and also from the excitation energies of these states, which lie close to the unperturbed energy (4.84 MeV) of the $(j_{15/2}, p_{1/2}^{-1})$ configuration, we assume that these states indeed contain a $(j_{15/2}, p_{1/2}^{-1})$ configuration and thus have one of the spins 7^+ or 8^+. The state observed at 4.602 MeV has previously been assigned as an 8^+ state.[32] No other states are observed in the spectra in the $j_{15/2}$ IAR, which is reasonable because of the small cross sections one expects for states with $p_{3/2}^{-1}$ and $f_{5/2}^{-1}$ configurations.

[32] J. Sandinos, G. Vallois, O. Beer, M. Gendrot, and P. Lopato, Phys. Letters **22**, 492 (1966).

V. CONCLUSION

The low-lying states of ^{208}Pb which have a $g_{9/2}$, $i_{11/2}$, or $j_{15/2}$ neutron coupled to various neutron holes ($p_{1/2}$, $f_{5/2}$, and $p_{3/2}$) have been investigated in the ^{208}Pb$(p, p')^{208}$Pb excitation function and angular distributions in the vicinity of the single-neutron IAR. The comparison of the observed decay widths with the theoretically calculated widths obtained from shell-model wave functions[5,6] gives fair agreement, but indicates that much more theoretical work is needed to describe these low-lying states correctly.

From the experimental angular distributions at the $g_{9/2}$ IAR and the partial widths obtained there from, the states with dominant $(g_{9/2}, p_{1/2}^{-1})$, $(g_{9/2}, f_{5/2}^{-1})$, and $(g_{9/2}, p_{3/2}^{-1})$ neutron configurations are determined. For states with known spins, such as the 3.469 MeV (4^-) and 3.702 MeV (5^-), an analysis of the angular distributions has yielded the wave-function coefficients for the various neutron-hole configurations. For the states with dominant $(g_{9/2}, p_{3/2}^{-1})$ configurations which lie between 4.15- and 4.8-MeV excitation, several spin assignments are suggested. The spin assignments are not completely unique, but are consistent with the expected sp widths given in Table III and the expected angular distributions.

For the $i_{11/2}$ IAR, no final-state spins are assigned. Two states are observed in the (p, p') reaction, however, which are not observed in the ^{207}Pb(d, p) reaction. These two states are likely to consist mainly of $(i_{11/2}, p_{3/2}^{-1})$ configurations. At the $j_{15/2}$ IAR, the same states are observed as in the ^{207}Pb(d, p) reaction.

Work which still remains to be done on these states is (1) to make spin assignments for the several unassigned states and to confirm the present spin assignments [the on-resonance $(p, p'\gamma)$ correlated and uncorrelated angular distributions measured with Ge(Li) γ detectors may give this information] and (2) to obtain accurate calculations of the single-particle widths, their exact energy dependence, and accurate calculations of the mixing phases. Several authors[33,34] are presently working on this problem. Zaidi, Dyer, and Coker have recently calculated wave functions for the IAR and the final ^{208}Pb states, using the same residual interaction, and are attempting to fit the measured angular distributions which are presented here.

ACKNOWLEDGMENTS

The authors wish to thank Professor J. S. Blair, Professor J. Bondorf, and Professor S. A. A. Zaidi for many stimulating discussions. The authors also wish to thank Miss S. Kellenbarger for supplying them with 3-mm detectors and Mrs. J. Sauer for preparing self-supporting Pb targets.

[33] J. S. Blair and G. Bund (private communication); W. Thompson and D. Robson (private communication).

[34] S. A. A. Zaidi, P. Dyer, and W. R. Coker, Bull. Am. Phys. Soc. **13**, 1463 (1968); P. Dyer and S. A. A. Zaidi, *ibid.* **13**, 1365 (1968).